

# Quantum circuit to estimate pi using quantum amplitude estimation

Takuma Noto

*Institute of Technology, Shimizu Corporation, 3-4-17, Etchujima, Koto-ku, Tokyo 135-8530, Japan*

*London Centre for Nanotechnology, University College London, 17-19 Gordon Street, London*

*WC1H 0AH, United Kingdom*

*Email: t.noto@shimz.co.jp*

## Abstract

This paper presents a quantum circuit for estimating pi value using arithmetic circuits and quantum amplitude estimation. We review and propose quantum multiplier and quantum squaring circuits as basic arithmetic circuits required for performing quantum computations. The multiplier, realized by using a quantum adder, is generalized to a set of binary numbers with varying number of digits. Especially, inputting two  $n$ -qubit binary numbers into the multiplier using a quantum adder with  $O(n)$  gates requires  $O(n^2)$  gates and at least ancillary qubits of  $n$ . The squarer can be implemented based on the multiplier. The squarer realized by a quantum adder requires the same order of gate size and ancillary qubits as its corresponding multiplier, while that realized by using quantum Fourier transform (QFT) requires  $O(n^3)$  gates without ancillary qubit. The proposed quantum circuit to estimate pi is based on Monte Carlo method and quantum amplitude estimation, which was implemented in  $4n + 1$  qubits at  $2^{2n}$  sampling by applying the QFT squarer. The proposed method was demonstrated using a quantum computer simulator with  $n$  being varied from 2 to 6, and the obtained result was compared with the one obtained by performing a classical calculation.

**Keyword:** Quantum circuit, Quantum multiplier accumulator, Quantum squarer, Quantum amplitude estimation, Monte Carlo method, Pi

## 1. Introduction

Quantum computers are expected to perform high-speed calculations in many fields. Recently, practical algorithms for Noisy Intermediate-Scale Quantum (NISQ) computer

that are based on the use of fewer qubits and fewer gates than the ideal ones for the future have been developed [1-3]. The Monte Carlo method on quantum computer by applying quantum amplitude estimation [4, 5] is one of the algorithms that have been reported to have less computational complexity than the classical methods [6]. Further, [5] demonstrated a quantum circuit for Monte Carlo integration of sine function by using a newly proposed quantum amplitude estimation method with few controlled-gate and no auxiliary qubits for NISQ.

Further, various small arithmetic operation circuits such as adder and multiplier (multiplier accumulator) are necessary when building a large circuit to solve a complex problem. An efficiently adder works as follows:  $|a\rangle|b\rangle \rightarrow |a\rangle|a+b\rangle$ , where  $|a\rangle$ ,  $|b\rangle$ , and  $|a+b\rangle$  are quantum registers with representative states of integer numbers  $a$ ,  $b$ , and  $a+b$ , respectively. This operation changes the state of the second register into  $|a+b\rangle$  even if  $|a\rangle$  and  $|b\rangle$  are a superposition of arbitrary integers.

Various quantum adders based on classical algorithm such as ripple-carry adder, carry look-ahead adder, or a combination of these algorithms have been implemented in quantum circuits [7, 8]. For example, a ripple-carry adder for two  $n$ -bit binary numbers can be implemented in  $O(n)$  gates without the use of an ancillary qubit [8]. As another approach, a quantum Fourier transform (QFT) based quantum adder can be implemented in  $O(n^2)$  gates with no ancillary qubit [9]. Quantum algorithms of a multiplier for two quantum registers have also been proposed [10-12]. Particularly, a QFT adder based multiplier consists of  $O(n^3)$  gates with no ancillary qubit [13-15].

In this paper, we first propose a classical and generalized digit by digit quantum multiplier based on quantum adder circuit and present a review of the QFT multiplier. Second, we propose two types of quantum squaring circuits based on the quantum multipliers. Finally, we demonstrate a quantum circuit to estimate pi by using the proposed quantum squarer and quantum amplitude estimation and compare the results obtained with the results obtained by performing a classical calculation.

## 2. Arithmetic circuit

### 2.1 Quantum multiplier

By inputting first quantum register  $|a\rangle_1 = |a_{n-1}\rangle_1 \otimes |a_{n-2}\rangle_1 \otimes \dots \otimes |a_0\rangle_1$  with  $n$ -qubit representing integer  $a = 2^{n-1}a_{n-1} + 2^{n-2}a_{n-2} + \dots + 2^0a_0$ , second quantum register  $|b\rangle_2 = |b_{m-1}\rangle_2 \otimes |b_{m-2}\rangle_2 \otimes \dots \otimes |b_0\rangle_2$  with  $m$ -qubit representing integer  $b = 2^{m-1}b_{m-1} + 2^{m-2}b_{m-2} + \dots + 2^0b_0$ , and third quantum register  $|c\rangle_3 = |c_{l-1}\rangle_3 \otimes |c_{l-2}\rangle_3 \otimes \dots \otimes |c_0\rangle_3$  with  $l$ -qubit representing integer  $c = 2^{l-1}c_{l-1} + 2^{l-2}c_{l-2} + \dots + 2^0c_0$ , a multiplier changes the third register as follows:

$$|a\rangle_1 |b\rangle_2 |c\rangle_3 \rightarrow |a\rangle_1 |b\rangle_2 |c + ab \bmod 2^l\rangle_3, \quad (1)$$

where the modulo in the third register on the right hand side implies that this operation may result in overflow when  $c + ab$  is more than  $2^l$ . Normally, there is no overflow when  $c = 0$  and  $l \geq m + n$ .

#### 2.1.1 Classical quantum multiplier

A digit by digit multiplication by applying an adder repeatedly is one of the classical algorithms for multiplying numbers. The quantum circuit of this classical algorithm, developed by using a weighted adder is shown in Fig. 1. The multiplier consists of controlled- $M_s$  ( $s = 0, 1, \dots, n-1$ ) gates as shown in Fig. 2. It takes inputs  $|a_s\rangle_1, |b\rangle_2, |c\rangle_3$ , and ancillary register  $|0\rangle_A = |0\rangle_A^{(m-1)} \otimes |0\rangle_A^{(m-2)} \otimes \dots \otimes |0\rangle_A^{(0)}$  with  $m$ -qubit. First, the product of  $a_s b_t$  ( $t = 0, 1, \dots, m-1$ ) is temporally stored in the  $t$ -th ancillary qubit as  $|0\rangle_A^{(t)} \rightarrow |a_s b_t\rangle_A^{(t)}$  by applying Toffoli gate (controlled-controlled-NOT gate) on  $|a_s\rangle_1$  and  $|b\rangle_2$  for control and on  $|0\rangle_A^{(t)}$  for the target. By applying a series of Toffoli gates before the weighted adder gate labeled  $2^s\Sigma$ , the ancillary register changes as follows:

$$|0\rangle_A \rightarrow |a_s b_{m-1}\rangle_A^{(m-1)} \otimes |a_s b_{m-2}\rangle_A^{(m-2)} \otimes \dots \otimes |a_s b_0\rangle_A^{(0)} = |a_s b\rangle_A. \quad (2)$$

Hence, applying weighted adder on  $|a_s b\rangle_A$  as addend and on  $|c\rangle_3$  as augend, the value stored in the third register changes as follows:

$$|c\rangle_3 \rightarrow |c + 2^s a_s b \bmod 2^l\rangle_3, \quad (3)$$

where weighted adder circuit can use an already-known quantum adder for two quantum registers that add  $|a_s b\rangle_A$  to the upper  $l - s$  digits of  $|c\rangle_3$  while the addend gets the factor  $2^s$ .

After applying the weighted adder, a series of Toffoli gates returns the state of the

ancillary register. Finally, by repeating controlled- $M_s$  gate for  $s = 0, 1, \dots, n - 1$ , the value stored in the third register changes as follows:

$$\begin{aligned}
 |c\rangle_3 &\rightarrow |c + 2^0 a_0 b \bmod 2^l\rangle_3 \\
 &\rightarrow |c + 2^1 a_1 b + 2^0 a_0 b \bmod 2^l\rangle_3 \\
 &\vdots \\
 &\rightarrow |c + 2^{n-1} a_{n-1} b + \dots + 2^1 a_1 b + 2^0 a_0 b \bmod 2^l\rangle_3 = |c + ab \bmod 2^l\rangle_3. \quad (4)
 \end{aligned}$$

This multiplier circuit consists of  $2mn$  Toffoli gate and  $n$  controlled- $M_s$  gate with  $m + N_A$  ancillary qubits. Herein,  $N_A$  denotes the number of ancillary qubits of the weighted adder. For two  $n$ -qubit multiplications that uses a weighted adder whose gate size is  $O(n)$  and no ancillary qubit, the multiplier can be implemented in  $O(n^2)$  gate with  $n$  ancillary qubits.

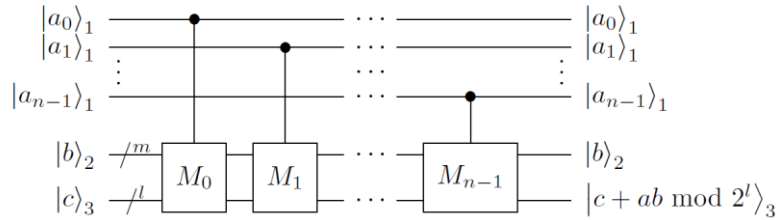


**Fig. 1** Quantum circuit of a quantum multiplier that uses a weighted adder. The circuit consists of a series of controlled- $M_s$  gates for  $s = 0, 1, \dots, n - 1$ .

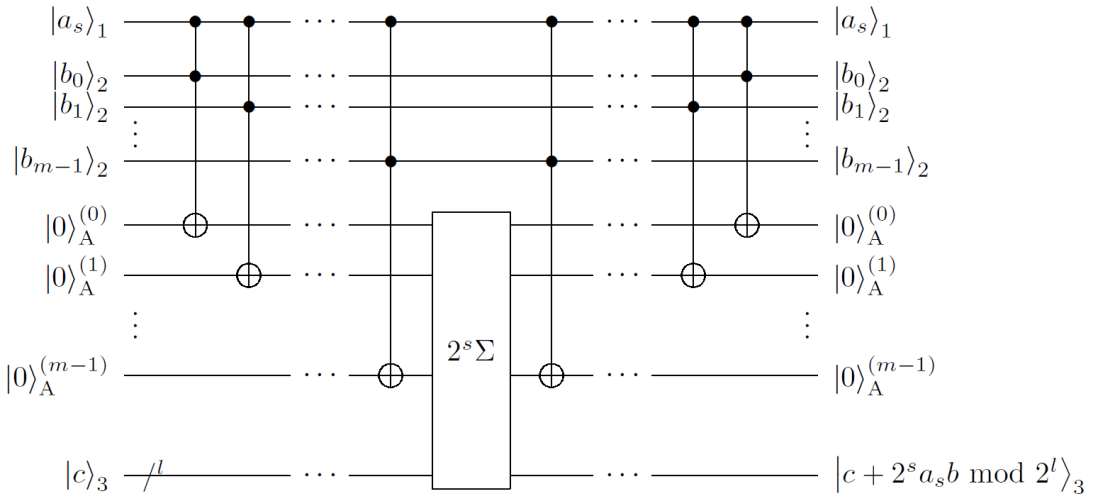


**Fig. 2** Quantum circuit of the controlled- $M_s$  gate.

### 2.1.2 QFT multiplier

QFT multiplier can be illustrated as shown in Fig. 3 with  $O(n^3)$  gates and no ancillary qubits [15]. First, QFT is applied to the third register and its state changes from  $|c\rangle_3 \rightarrow |\varphi(c)\rangle_3$ , where  $u$ -th ( $u = 0, 1, \dots, l-1$ ) qubit of the third register changed by QFT can be expressed as follows:

$$|c_u\rangle_3 \rightarrow \frac{1}{\sqrt{2}}(|0\rangle_3 + e^{2\pi i 0 \cdot c_u c_{u-1} \dots c_0} |1\rangle_3) = |\varphi_u(c)\rangle_3. \quad (5)$$

Then, the phase of the third register is rotated by applying controlled- $2^s \Sigma_p$  gate, which acts on  $|a_s\rangle_1$  as control and on  $|b\rangle_2$  and  $|\varphi(c)\rangle_3$  as input. The circuit of the gate consists of a series of a controlled-controlled- $R_j$  gate that acts on  $|a_s\rangle_1$  and  $|b_t\rangle_2$  as control, and rotate the  $u$ -th qubit of the third register with  $j = -s - t + u + 1$  as shown in Fig. 4, where  $R_j$  gate can be expressed as follows:

$$R_j = \begin{pmatrix} 1 & 0 \\ 0 & e^{\frac{2\pi i}{2^j}} \end{pmatrix}. \quad (6)$$

Hence, the  $R_j$  gate will be an identity operator when  $j \leq 0$ .

Now, non-controlled  $2^0 \Sigma_p$  operations when  $s = 0$  are equal to phase rotations of the QFT adder [9] that change the value in the third register as follows:  $|\varphi(c)\rangle_3 \rightarrow |\varphi(c + b \bmod 2^l)\rangle_3$ . Controlled  $2^s \Sigma_p$  operation with  $|a_s\rangle_1$  as control, further multiplies the phase of  $2^s a_s$  and the third register changes as follows:  $|\varphi(c)\rangle_3 \rightarrow |\varphi(c + 2^s a_s b \bmod 2^l)\rangle_3$ . Thus, the third register changes in the following manner by repeating controlled- $2^s \Sigma_p$  gate for  $s = 0, 1, \dots, n-1$ .

$$\begin{aligned} |\varphi(c)\rangle_3 &\rightarrow |\varphi(c + 2^0 a_0 b \bmod 2^l)\rangle_3 \\ &\rightarrow |\varphi(c + 2^1 a_1 b + 2^0 a_0 b \bmod 2^l)\rangle_3 \\ &\quad \vdots \\ &\rightarrow |\varphi(c + 2^{n-1} a_{n-1} b + \dots + 2^1 a_1 b + 2^0 a_0 b \bmod 2^l)\rangle_3 \\ &= |\varphi(c + ab \bmod 2^l)\rangle_3. \end{aligned} \quad (7)$$

Finally, the third register is transformed by using inversed-QFT to attain the state  $|c + ab \bmod 2^l\rangle_3$ .

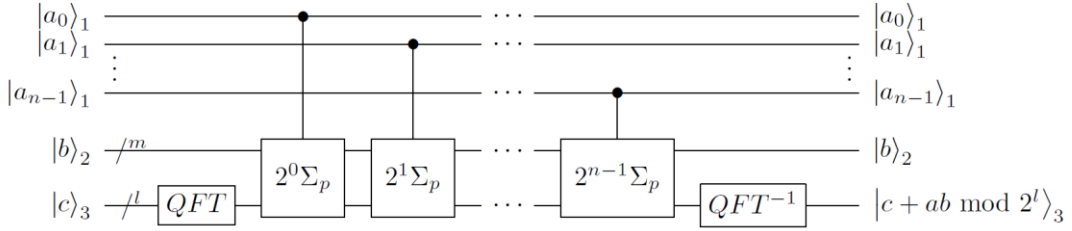


**Fig. 3** Quantum circuit of QFT multiplier consisting of a series of controlled- $2^s\Sigma_p$  gates for  $s = 0, 1, \dots, n - 1$ . In the circuit,  $QFT$  and  $QFT^{-1}$  stand for the QFT circuit and its inverse circuit, respectively.

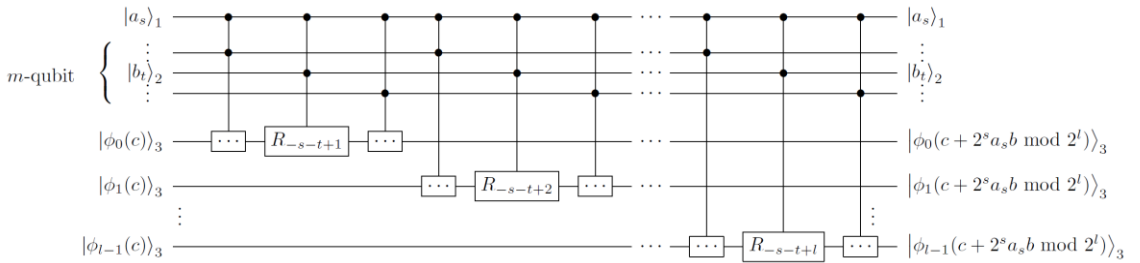


**Fig. 4** Quantum circuit of controlled- $2^s\Sigma_p$  gate.

## 2.2 Quantum squarer

A squaring circuit is used to calculate the squared number of integers in the superposition. The circuits can be implemented similarly as the multiplier, by omitting one of its inputs. Inputting the first quantum register  $|a\rangle_1$  with  $n$ -qubit and the second quantum register  $|b\rangle_2$  with  $m$ -qubit, a squarer circuit changes the second register as follows:

$$|a\rangle_1|b\rangle_2 \rightarrow |a\rangle_1|b + a^2 \bmod 2^m\rangle_2, \quad (8)$$

where the modulo in the second register on the right hand side signifies that an overflow may occur when  $b + a^2$  is more than  $2^m$ . Normally, there is no overflow when  $b = 0$  and  $m \geq 2n$ .

### 2.2.1 Classical quantum squarer

The quantum squarer circuit shown in Fig. 5 uses weighted adder and consists of series of  $S_s$  ( $s = 0, 1, \dots, n - 1$ ) gates as shown in Fig. 6 with inputs  $|a\rangle_1$  and  $|b\rangle_2$  and ancillary quantum register  $|0\rangle_A$  with  $n$ -qubit. In  $S_s$  gate, the  $s$ -th qubit of the ancillary quantum register changes as follows:  $|0\rangle_A^{(s)} \rightarrow |a_s\rangle_A^{(s)} = |a_s^2\rangle_A^{(s)}$  by applying a controlled-NOT

(CNOT) gate on  $|a_s\rangle_1$  and  $|0\rangle_A^{(s)}$  as control and target qubits, respectively. Herein,  $a_s$  only take 0 or 1 and  $a_s^2$  is equal to  $a_s$ . The  $t$ -th ( $t = 0, 1, \dots, n-1, t \neq s$ ) qubit of the ancillary quantum register changes as follows:  $|0\rangle_A^{(t)} \rightarrow |a_s a_t\rangle_A^{(t)}$  by applying Toffoli gate on  $|a_s\rangle_1$  and  $|a_t\rangle_1$  as control and on  $|0\rangle_A^{(t)}$  as a target. After applying a series of Toffoli gates and CNOT gate, the state of the ancillary quantum register becomes  $|a_s a_{n-1}\rangle_A^{(n-1)} \otimes |a_s a_{n-2}\rangle_A^{(n-2)} \otimes \dots \otimes |a_s a_0\rangle_A^{(0)} = |a_s a\rangle_A$ . Thus, applying weighted adder labeled  $2^s\Sigma$  on  $|a_s a\rangle_A$  as addend and on  $|b\rangle_2$  as augend as well as a quantum multiplier as presented in section 2.1.1, the state of the second register becomes  $|b + 2^s a_s a \bmod 2^m\rangle_2$ . Finally, the ancillary quantum register is set back to  $|0\rangle_A$  by using a series of controlled-gate while the state of the second register becomes  $|b + a^2 \bmod 2^m\rangle_2$  by applying a series of  $S_s$  gate.

This quantum squarer consists of  $2n$  CNOT gates,  $2(n^2 - n)$  Toffoli gates, and  $n$   $2^s\Sigma$  gate with  $n + N_A$  ancillary qubits. The order of its gate size and ancillary qubits is equal to that of a quantum multiplier for two  $n$ -qubit binary numbers presented in section 2.1.1.

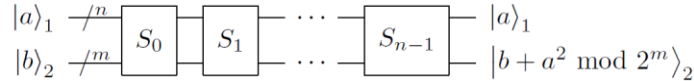


**Fig. 5** Quantum circuit of quantum squarer obtained by using weighted adder consisting of a series of  $S_s$  gates, where  $s = 0, 1, \dots, n-1$ .

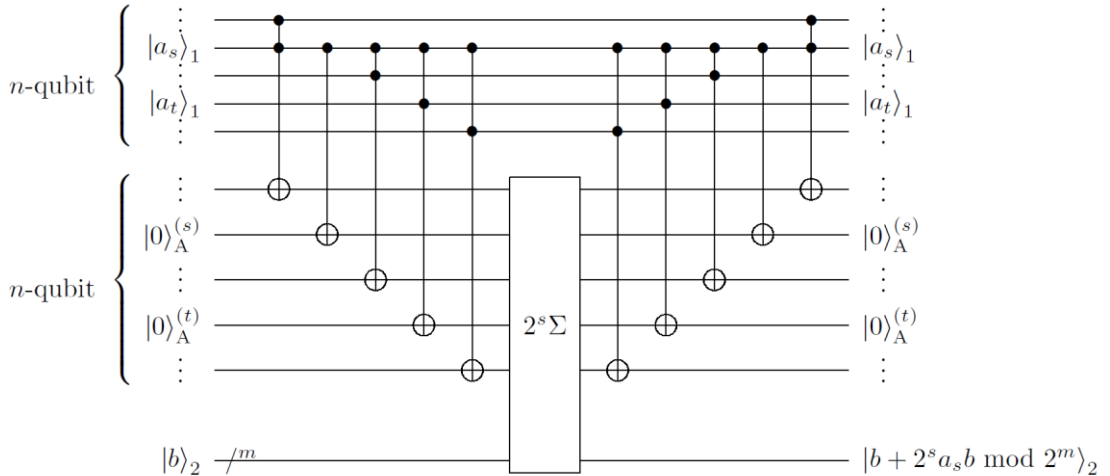


**Fig. 6** Quantum circuit of  $S_s$  gate.

### 2.2.2 QFT squarer

A QFT based quantum squarer is shown in Fig. 7. First, the second quantum register  $|b\rangle_2$  is translated to  $|\varphi(b)\rangle_2$  by QFT, where the  $u$ -th ( $u = 0, 1, \dots, m-1$ ) qubit of the second register changes as follows:

$$|b_u\rangle_2 \rightarrow \frac{1}{\sqrt{2}} (|0\rangle_2 + e^{2\pi i 0.b_u b_{u-1} \dots b_0} |1\rangle_2) = |\varphi_u(b)\rangle_2. \quad (9)$$

Then, a series of  $2^s \Sigma_{p,s}$  gate inputting  $|a\rangle_1$  and  $|\varphi(b)\rangle_2$  rotate the second register by an encoded value of  $2^s a_s a$ . The  $u$ -th qubit of the second register is rotated by controlled-controlled- $R_{-s-t+u+1}$  gate (which is controlled by  $|a_s\rangle_1$  and  $|a_t\rangle_1$  ( $t = 0, 1, \dots, n-1, t \neq s$ )) and by controlled- $R_{-2s+u+1}$  gate (which is controlled by  $|a_s\rangle_1$ ) as shown in Fig. 8. The  $2^s \Sigma_{p,s}$  gate changes the second quantum register as follows:  $|\varphi(b)\rangle_2 \rightarrow |\varphi(b + 2^s a_s a \bmod 2^m)\rangle_2$ , and a series of the  $2^s \Sigma_{p,s}$  gates change it as follows:  $|\varphi(b)\rangle_2 \rightarrow |\varphi(b + a^2 \bmod 2^m)\rangle_2$ .

This QFT squarer requires  $O(n^3)$  gate size with no ancillary qubits as well as QFT multiplier.

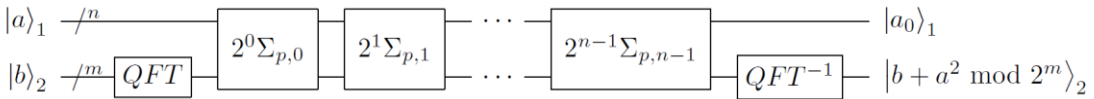


**Fig. 7** Quantum circuit of QFT squarer consisting of a series of  $2^s \Sigma_{p,s}$  gates where  $s = 0, 1, \dots, n-1$ .

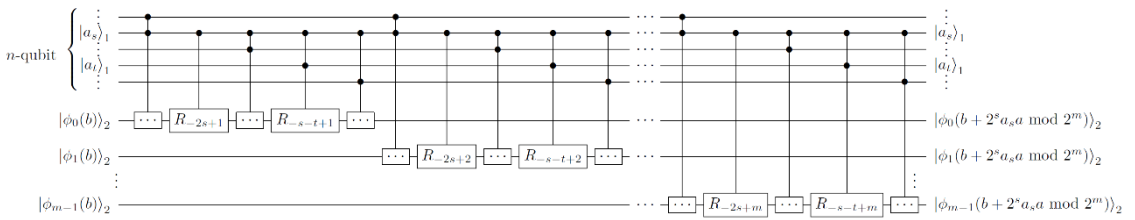


**Fig. 8** Quantum circuit of  $2^s \Sigma_{p,s}$  gate.

## 3. Quantum circuit to estimate pi

### 3.1 Preparation

The Monte Carlo method in classical computers solves a problem by using random number such as estimating the expected value of a problem by using repeated random sampling. The accuracy of the result obtained in such a task can be improved by

increasing the computational complexity or number of samplings, which require  $O(1/\epsilon^2)$  to produce an estimated error  $\epsilon$ .

In quantum computing, new algorithms have been proposed for evaluating the expected value through quantum amplitude estimation [6]. Suppose  $f(x)$  is a classical real value function for  $n$ -bit binary input  $x \in \{0, 1\}^n$  and  $p(x)$  is its probability, the expected value of all possible numbers in  $x$  can be evaluated as follows:

$$\mathbb{E}[f(x)] = \sum_{x=0}^{2^n-1} f(x) p(x). \quad (10)$$

Let a unitary operator  $R$  is defined to act on the first register  $|x\rangle_1$  with  $n$ -qubit and auxiliary second register  $|0\rangle_2$  with 1-qubit to rotate the second register when  $f(x)$  is bounded between 0 and 1 as follows:

$$R|x\rangle_1|0\rangle_2 = \sqrt{f(x)}|x\rangle_1|1\rangle_2 + \sqrt{1-f(x)}|x\rangle_1|0\rangle_2. \quad (11)$$

Let unitary operation  $P$  be an operation for building a superposition of all  $x$  states from  $|0\rangle_1$  state as follows:

$$P|0\rangle_1 = \sum_{x=0}^{2^n-1} \sqrt{p(x)}|x\rangle_1. \quad (12)$$

Then, by applying operator  $P$  and  $R$  to the initialized quantum registers, the expected value appears as a probability of measuring  $|1\rangle_2$  in the second register as follows:

$$R(P \otimes I_2)|0\rangle_1|0\rangle_2 = \sum_{x=0}^{2^n-1} \sqrt{f(x)}\sqrt{p(x)}|x\rangle_1|1\rangle_2 + \sum_{x=0}^{2^n-1} \sqrt{1-f(x)}\sqrt{p(x)}|x\rangle_1|0\rangle_2, \quad (13)$$

where  $I_2$  denotes an identity operator on the second register. Therefore, the expected value can be estimated by amplitude estimation in the state where the second register is  $|1\rangle_2$ . The total number of times of calling the operation  $A=R(P \otimes I_2)$  and  $A^{-1}$  require  $O(1/\epsilon)$  in the quantum amplitude estimation, which squares faster than a classical Monte Carlo method [6].

### 3.2 Quantum circuit

$\pi$  can be estimated from the area ratio of a square and a quadrant inscribed in a square whose radius is equal to the side length of the square, which is a popular algorithm. By preparing  $n$ -qubit registers to build superposition of integers representing binary numbers

on  $x$  and  $y$  axes, respectively, a total of  $2^{2n}$  points in a square with a side length of  $2^n$  can be sampled as shown in Fig. 9. The function that determines whether the sampled point  $(x, y)$  is inside the quadrant or not is as follows:

$$f(x, y) = \begin{cases} 1 & \text{if } x^2 + y^2 < 2^{2n} \\ 0 & \text{if } x^2 + y^2 \geq 2^{2n} \end{cases}. \quad (14)$$

Herein,  $\pi$  can be estimated as follows:

$$\frac{\pi}{4} = \sum_{y=0}^{2^n-1} \sum_{x=0}^{2^n-1} f(x, y) p(x, y), \quad (15)$$

where  $p(x, y)$  denotes the probability of sampling point  $(x, y)$ .

In the quantum circuit, three quantum registers are used to estimate  $\pi$ : the first quantum register with  $n$ -qubit for sampling along the  $x$ -axis, the second quantum register with  $n$ -qubit for sampling along the  $y$ -axis, and the third quantum register with 1-qubit for amplitude estimation. Thus, the operator  $P$  and  $R$  in this algorithm act on two and three quantum registers, respectively, as follows:

$$\begin{aligned} R(P \otimes I_3) |0\rangle_1 |0\rangle_2 |0\rangle_3 &= R \sum_{y=0}^{2^n-1} \sum_{x=0}^{2^n-1} \sqrt{p(x, y)} |x\rangle_1 |y\rangle_2 |0\rangle_3 \\ &= \sum_{y=0}^{2^n-1} \sum_{x=0}^{2^n-1} \sqrt{f(x, y)} \sqrt{p(x, y)} |x\rangle_1 |y\rangle_2 |1\rangle_3 \\ &\quad + \sum_{y=0}^{2^n-1} \sum_{x=0}^{2^n-1} \sqrt{1 - f(x, y)} \sqrt{p(x, y)} |x\rangle_1 |y\rangle_2 |0\rangle_3, \end{aligned} \quad (16)$$

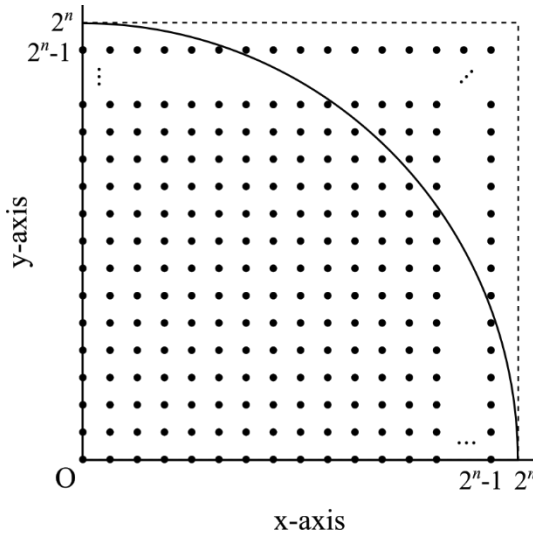
where  $I_3$  denotes an identify operation on the third quantum register. Hence,  $\pi$  can be estimated by using the quantum amplitude estimation method when the third register is  $|1\rangle_3$ .

The operation  $P$  builds superposition of  $x$  and  $y$  with the same probability, and it is implemented by applying Hadamard gates on each qubit of the first and second registers.

The operation  $R$  rotates the third register according to the state of the first and second registers and the amplitude become  $\sqrt{f(x, y)}$  when the state is  $|1\rangle_3$ . Further, this rotated state can be represented as follows since  $f(x, y)$  takes only 0 or 1:

$$\sqrt{f(x, y)} |1\rangle_3 + \sqrt{1 - f(x, y)} |0\rangle_3 = |f(x, y)\rangle_3. \quad (17)$$

The operation  $R$  implemented in a quantum circuit is shown in Fig. 10. This circuit requires an ancillary quantum register with  $2n$ -qubit initialized to  $|0\rangle_A$ . First, the ancillary quantum register is combined with the third quantum register so that the third register is the most significant bit, which is referred to as 3A register. Then, squared values of  $x$  and  $y$  are added in the 3A register by quantum squarer proposed in section 2.2. When the 3A register is split into original 1 and  $2n$  qubits, the state is represented as  $|\overline{f(x,y)}\rangle_3|x^2 + y^2 \bmod 2^{2n}\rangle_A$  because the third quantum register gets  $|1\rangle_3$  only if  $x^2 + y^2$  is more than  $2^{2n}$ . By attaching the X gate to the third quantum register, the state become  $|f(x,y)\rangle_3$ . The ancillary quantum register can be undone by performing inverse quantum squarer operation because quantum squarer is a unitary operation. These operations are summarized as follows:

$$\begin{aligned}
 & |x\rangle_1|y\rangle_2|0\rangle_3|0\rangle_A \\
 \rightarrow & |x\rangle_1|y\rangle_2|0\rangle_{3A} && \text{Combining 3rd and ancillary register} \\
 \rightarrow & |x\rangle_1|y\rangle_2|x^2 + y^2 \bmod 2^{2n+1}\rangle_{3A} && \text{Squaring } x \text{ and } y \\
 \rightarrow & |x\rangle_1|y\rangle_2|\overline{f(x,y)}\rangle_3|x^2 + y^2 \bmod 2^{2n}\rangle_A && \text{Spliting 3A register} \\
 \rightarrow & |x\rangle_1|y\rangle_2|f(x,y)\rangle_3|x^2 + y^2 \bmod 2^{2n}\rangle_A && \text{NOT opeartion on 3rd register} \\
 \rightarrow & |x\rangle_1|y\rangle_2|f(x,y)\rangle_3|0\rangle_A && \text{Undoing ancillary register}
 \end{aligned}$$


**Fig. 9** Sampling points in a squarer with a side length of  $2^n$  and an inscribed quadrant.

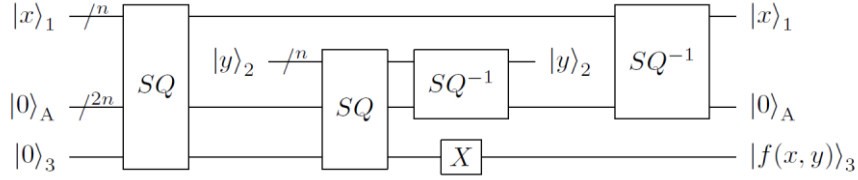


**Fig. 10** Quantum circuit of operation  $R$  to estimate pi. In the circuit,  $SQ$  and  $SQ^{-1}$  refer to the quantum squarer circuit and its inverse circuit, respectively.

### 3.3 Simulation

We implemented the quantum circuit to estimate pi in Qiskit 0.19.2 [16, 17] and performed the simulation using its quantum computer simulator. The QFT squarer proposed in section 2.2.2 and quantum amplitude estimation method using maximum likelihood [5] (to avoid increasing the ancillary qubits) were used in the circuit. The total number of qubits including ancillary qubits is  $4n + 1$  while the total number of sampling is  $2^{2n}$ .

The computational complexity of the quantum amplitude estimation method is defined by the total number of calling the operation  $A = R(P \otimes I_3)$  and  $A^{-1}$ , and that of using maximum likelihood is  $O((1/\epsilon_A) \ln(1/\epsilon_A))$ , where  $\epsilon_A$  is the estimation error of the quantum amplitude estimation. The method estimates the quantum amplitude by applying an operator including the  $A$  and  $A^{-1}$  for  $m_k$  times and by using maximum likelihood on multiple circuit sets with different  $k$ . The simulations were performed for two patterns:  $k_{\max} = 1$  and  $5$ , which are circuit sets with  $k = 0$  to  $k_{\max}$  with  $m_0 = 0$  and  $m_k = 2^{k-1}$ . For the 100 shots per circuit, the computational complexity of the former is 400 and  $\epsilon_A$  is  $O(10^{-2})$ , while it is 6,800 and  $O(10^{-3})$  for the later.

During the simulation, pi was estimated 100 times for each  $n$  while  $n$  was varied from 2 to 6 and the averaged values and standard deviations of pi were recorded. Additionally, the expected values obtained by using systematic samplings were calculated by performing classical calculations.

### 3.4 Results and discussion

A plot of the average estimated values and standard deviations obtained from the quantum simulations and the expected value obtained through classical calculations is shown in Fig. 11. The results of quantum simulations are in line with those obtained by performing classical calculations. However, errors  $\epsilon_S$  from the sampling numbers chosen have to be considered to estimate pi. While the number of samples and the computational complexity are the same in classical Monte Carlo method, they are different in the quantum circuit. The  $\epsilon_S$  is  $O(1/\sqrt[d]{N})$ , where  $d$  denotes the dimension of the problem and  $N$  denotes the total number of samples. In the case of pi estimation,  $\epsilon_S$  is  $O(1/2^n)$  and the total estimation error is  $\epsilon_S + \epsilon_A$ . The computational complexity can be decreased by using original quantum amplitude estimation of  $O(1/\epsilon_A)$  [5], the number of qubits used for sampling in each dimension is expected to require  $O(\log_2(1/\epsilon_A))$  or more to produce sufficient accuracy.

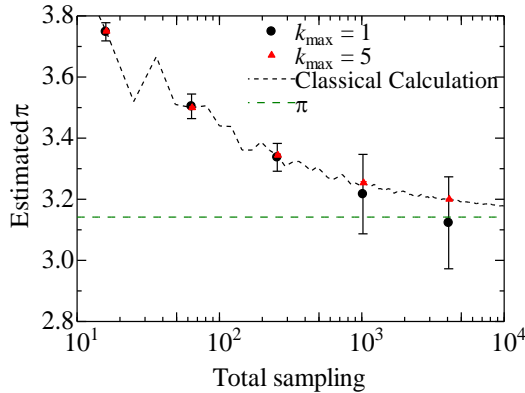


**Fig. 11** Estimated pi from the quantum simulations and classical calculation

## 4. Conclusion

In this paper, quantum circuits for multiplying, squaring, and estimating pi are proposed. The proposed quantum multiplier can be used to calculate different digits of binary numbers by using known quantum adder. In the case of multiplication of two  $n$ -qubit binary numbers using quantum adder with gate size of  $O(n)$ , the multiplier requires  $O(n^2)$  gate and at least  $n$  ancillary qubits while known QFT multiplier requires  $O(n^3)$  gate without any ancillary qubits.

Two types of quantum multiplier based quantum squarers are also proposed, which reduce input quantum register while requiring the same order of gate size and ancillary qubits as the quantum multiplier.

A quantum algorithm to estimate pi based on Monte Carlo method and quantum amplitude estimation was implemented and demonstrated using a quantum computer simulator. This circuit required  $4n + 1$  qubits for a total of  $2^{2n}$  sampling size. The estimated values contain  $\epsilon_S$  and  $\epsilon_A$  errors, which are caused by the sampling number chosen and computational complexity, respectively. To obtain higher accuracy, the circuit requires an adequate number of qubits for sampling that corresponds to the computational complexity.

## Acknowledgements

The author thanks Prof. Sougato Bose and Dr. Hidekazu Kurebayashi from University College London for their support and advice.

## Reference

1. Farhi, E., Goldstone, J., Gutmann, S.: A quantum approximate optimization algorithm. arXiv:1411.4028 [quant-ph]. (2014)
2. Peruzzo, A., McClean, J., Shadbolt, P., Yung, M.-H., Zhou, X.-Q., Love, P.J., Aspuru-Guzik, A., O’Brien, J.L.: A variational eigenvalue solver on a photonic quantum processor. *Nat. Comm.* 5, 4213 (2014)
3. Mitarai, K., Negoro, M., Kitagawa, M., Fujii, K.: Quantum circuit learning. *Phys. Rev. A.* 98, 032309 (2018)
4. Brassard, G., Hoyer, P., Mosca, M., Tapp, A.: Quantum amplitude amplification and estimation. *AMS Contemporary Mathematics.* 305, 53–74 (2002)
5. Suzuki, Y., Uno, S., Raymond, R., Tanaka, T., Onodera, T., Yamamoto, N.: Amplitude estimation without phase estimation. *Quantum Inf. Process.* 19, 75 (2020)
6. Montanaro, A.: Quantum speedup of Monte Carlo methods. *P. Roy. Soc. A-Math Phy.* 471, 20150301 (2015)
7. Vedral, V., Barenco, A., Ekert, A.: Quantum networks for elementary arithmetic operations. *Phys. Rev. A.* 54, 147–153 (1996)
8. Takahashi, Y., Tani, S., Kunihiro, N.: Quantum addition circuits and unbounded fan-out. *Quantum Info. Comput.* 10, 872–890 (2010)
9. Draper, T.G.: Addition on a quantum computer. arXiv:quant-ph/0008033. (2000)

10. Álvarez-Sánchez, J.J., Álvarez-Bravo, J.V., Nieto, L.M.: A quantum architecture for multiplying signed integers. *J. Phys.: Conf. Ser.* 128, 012013 (2008)
11. Kotiyal, S., Thapliyal, H., Ranganathan, N.: Circuit for reversible quantum multiplier based on binary tree optimizing ancilla and garbage bits. In: 2014 27th International Conference on VLSI Design and 2014 13th International Conference on Embedded Systems. pp. 545–550 (2014)
12. Babu, H.Md.H.: Cost-efficient design of a quantum multiplier–accumulator unit. *Quantum Inf. Process.* 16, 30 (2016)
13. Maynard, C.M., Pius, E.: A quantum multiply-accumulator. *Quantum Inf. Process.* 13, 1127–1138 (2014)
14. Pavlidis, A., Gizopoulos, D.: Fast quantum modular exponentiation architecture for Shor’s factoring algorithm. *Quantum Info. Comput.* 14, 649–682 (2014)
15. Ruiz-Perez, L., Garcia-Escartin, J.C.: Quantum arithmetic with the quantum Fourier transform. *Quantum Inf. Process.* 16, 152 (2017)
16. Aleksandrowicz, G., Alexander, T., Barkoutsos, P., Bello, L., Ben-Haim, Y., Bucher, D., Cabrera-Hernández, F.J., Carballo-Franquis, J., Chen, A., Chen, C.F., Chow, J.M., Córcoles-Gonzales, A.D., Cross, A.J., Cross, A., Cruz-Benito, J., Culver, C., González, S.D.L.P., Torre, E.D.L., Ding, D., Dumitrescu, E., Duran, I., Eendebak, P., Everitt, M., Sertage, I.F., Frisch, A., Fuhrer, A., Gambetta, J., Gago, B.G., Gomez-Mosquera, J., Greenberg, D., Hamamura, I., Havlicek, V., Hellmers, J., Herok, Ł., Horii, H., Hu, S., Imamichi, T., Itoko, T., Javadi-Abhari, A., Kanazawa, N., Karazeev, A., Krsulich, K., Liu, P., Luh, Y., Maeng, Y., Marques, M., Martín-Fernández, F.J., McClure, D.T., McKay, D., Meesala, S., Mezzacapo, A., Moll, N., Rodríguez, D.M., Nannicini, G., Nation, P., Ollitrault, P., O’Riordan, L.J., Paik, H., Pérez, J., Phan, A., Pistoia, M., Prutyanov, V., Reuter, M., Rice, J., Davila, A.R., Rudy, R.H.P., Ryu, M., Sathaye, N., Schnabel, C., Schoute, E., Setia, K., Shi, Y., Silva, A., Siraichi, Y., Sivarajah, S., Smolin, J.A., Soeken, M., Takahashi, H., Tavernelli, I., Taylor, C., Taylour, P., Trabing, K., Treinish, M., Turner, W., Vogt-Lee, D., Vuillot, C., Wildstrom, J.A., Wilson, J., Winston, E., Wood, C., Wood, S., Wörner, S., Akhalwaya, I.Y., Zoufal, C.: Qiskit: An open-source framework for quantum computing. (2019). <https://doi.org/10.5281/zenodo.2562110>
17. Gambetta, J., Treinish, M., Kassebaum, P., Nation, P., Rodríguez, D.M., González, S.D.L.P., Hu, S., Krsulich, K., Zdanski, L., qiskit-bot, Yu, J., Travis-S-IBM, Gomez, J., McKay, D., Gacon, J., Naveh, Y., Wood, S., lerongil, Capelluto, L., Ishizaki, K., abbycross, tigerjack, Garion, S., Dague, S., RohitMidha23, Marques, M., GEORGE,

M., Swarm, J., AlbinoZenci, Cruz, A.:Qiskit/qiskit: Qiskit 0.19.2. (2020).  
<https://doi.org/10.5281/zenodo.3829023>